Ital. J. Geosci., Vol. 137 (2018), pp. 465-477, 9 figs., 2 tabs. (https://doi.org/10.3301/IJG.2018.20)

$^{98}Mo/^{95}Mo$ and $^{238}U/^{235}U$ in lamproites, shoshonites, and high-K calc-alkaline rocks from Western Alps: inferences on their genesis

Martina Casalini

ABSTRACT

Oligocene ultrapotassic and associated potassic rocks from Western Alps derived from the crystallisation of magmas originated from partial melting of mantle sources extremely enriched in recycled crustal components. These rocks are well suited for studying the effects of subduction-related, sediment-derived metasomatism on Molybdenum and Uranium isotopes. This paper reports the first $^{98}Mo/^{95}Mo$ and $^{238}U/^{235}U$ data on potassic and ultrapotassic rocks at destructive plate margins. Both $^{98}Mo/^{95}Mo$ and $^{238}U/^{235}U$ ratios show large variations in the samples from Western Alps. U isotope compositions are consistent with an increasing role of metasomatising melts from recycled sediments, which explains the variable enrichment in potassium and incompatible trace elements passing from high-K calc-alkaline to lamproitic magmas through shoshonitic ones. The variation of Mo isotope compositions is more complex due to the extreme depletion in Mo observed and since their values exceed the range observed for volcanic arcs. These features were investigated considering several possible processes such as secondary weathering, hosting of Mo related to residual mineral phases during sediment melting or physical removal during subduction. The results were also discussed in the framework of the complex processes responsible for the genesis and geochemical characteristics of the Tethyan Realm Lamproites, particularly in relationship with the exotic SALATHO geochemical component.

Keywords: *Molybdenum isotopes, Uranium isotopes, Western Alps, lamproites, shoshonites.*

INTRODUCTION

The Alpine chain is the westernmost portion of a continuous orogenic belt (Fig. 1) extending to the Himalaya and Tibet formed during the Alpine orogenesis and related with the closure of the Tethys and its branches, as a consequence of the diachronous collisions of Gondwana-derived lithospheric plates started on Early Permian (e.g., Tommasini *et alii*, 2011). The long-lasting subduction of the different Tethyan realm oceans, together with the diachronous collisions, was accompanied by long-lived magmatic activity characterised by calc-alkaline to shoshonites, usually associated to ultrapotassic subduction-related suites, which in some cases are represented by lamproites (e.g., Benito *et alii*, 1999; Turner *et alii*, 1999; Altherr *et alii*, 2004, 2008; Prelević *et alii*, 2004, 2005; Gao *et alii*, 2007; Conticelli *et alii*, 2009; Tommasini *et alii*, 2011; Krmíček *et alii*, 2016; Soder *et alii*, 2016). Lamproites are a peculiar family of low-Ca and -Al ultrapotassic rocks (Foley *et alii*, 1987) that can be found either in within-plate tectonic setting or at destructive plate margins (Bergman, 1987; Mitchell & Bergman, 1991). In both cases lamproites are characterised by an extraordinary high concentration of incompatible trace elements, higher than most crustal rocks, so that crustal contamination would dilute rather than enrich their contents in ultrapotassic magmas (e.g., Conticelli, 1998; Murphy *et alii*, 2002). Subduction-related lamproites differ from within-plate ones in terms of trace element distribution, with depletion of High Field Strength (HFS) elements (except Th) with respect to Large Ion Lithophile (LIL) ones, and by extremely radiogenic Sr and unradiogenic Nd ($^{87}Sr/^{86}Sr$ 0.70380 - 0.73629 and $^{143}Nd/^{144}Nd$ 0.51180 - 0.51252, respectively), and distinctive Hf and Pb isotopes ($^{176}Hf/^{177}Hf$ 0.282327 - 0.282789 and $^{206}Pb/^{204}Pb$ 18.409 - 18.930, respectively) (e.g., Fraser *et alii*, 1985; Peccerillo *et alii*, 1988; Nelson *et alii*, 1986; Conticelli & Peccerillo, 1992; Conticelli *et alii*, 1992, 2002, 2004, 2007, 2009, 2010, 2013, 2015; Carlson & Irving, 1994; Mirnejad & Bell, 2006; Prelević *et alii*, 2008, 2010; Avanzinelli *et alii*, 2009; Tommasini *et alii*, 2011). These peculiar characters reflect a dominance of lithospheric mantle contaminated by subducted crust-derived sediments (Conticelli & Peccerillo, 1992; Peccerillo *et alii*, 1988; Prelević *et alii*, 2008, 2010).

Lamproitic rocks are thought to result from a multi-stage process affecting the mantle sources including an episode of extreme depletion, followed one of enrichment through addition of a recycled, subduction-derived, crustal component (i.e., terrigenous sediments with different age and provenance), and finally interaction with melts from the convecting mantle (Conticelli *et alii*, 1992, 2004, 2007, 2009, 2010, 2013, 2015; Peccerillo *et alii*, 1988; Prelević *et alii*, 2008, 2010; Avanzinelli *et alii*, 2009; Tommasini *et alii*, 2011; Peccerillo & Frezzotti, 2015).

These complex processes produce a mantle source made up by phlogopite-pyroxenitic veins enclosed within the lithospheric mantle (Foley, 1992). Melting of such a metasomatised mantle source at variable degrees, during post-collisional tectonics, is able to generate a broad spectrum of different magmas: when melting of veins dominates lamproitic magmas are produced, whereas as the vein melt is diluted by increasing partial melting of the surrounding peridotite shoshonitic, high-K and calc-alkaline magmas are generated (Foley, 1992; Prelević *et alii*, 2008; Conticelli *et alii*, 2007, 2009, 2015).

In the Western Alps dikes and lavas, spanning in geochemical affinity from lamproites through shoshonitic to high-K calc-alkaline, were emplaced during Oligocene (e.g.,

Dipartimento di Scienze della Terra, Università degli Studi di Firenze, via Giorgio La Pira 4, I-50121, Firenze, Italy.
Bristol Isotope Group, School of Earth Sciences, University of Bristol, Queens Road, Bristol BS8 1RJ, UK.
Corresponding author e-mail: martina.casalini@unifi.it.

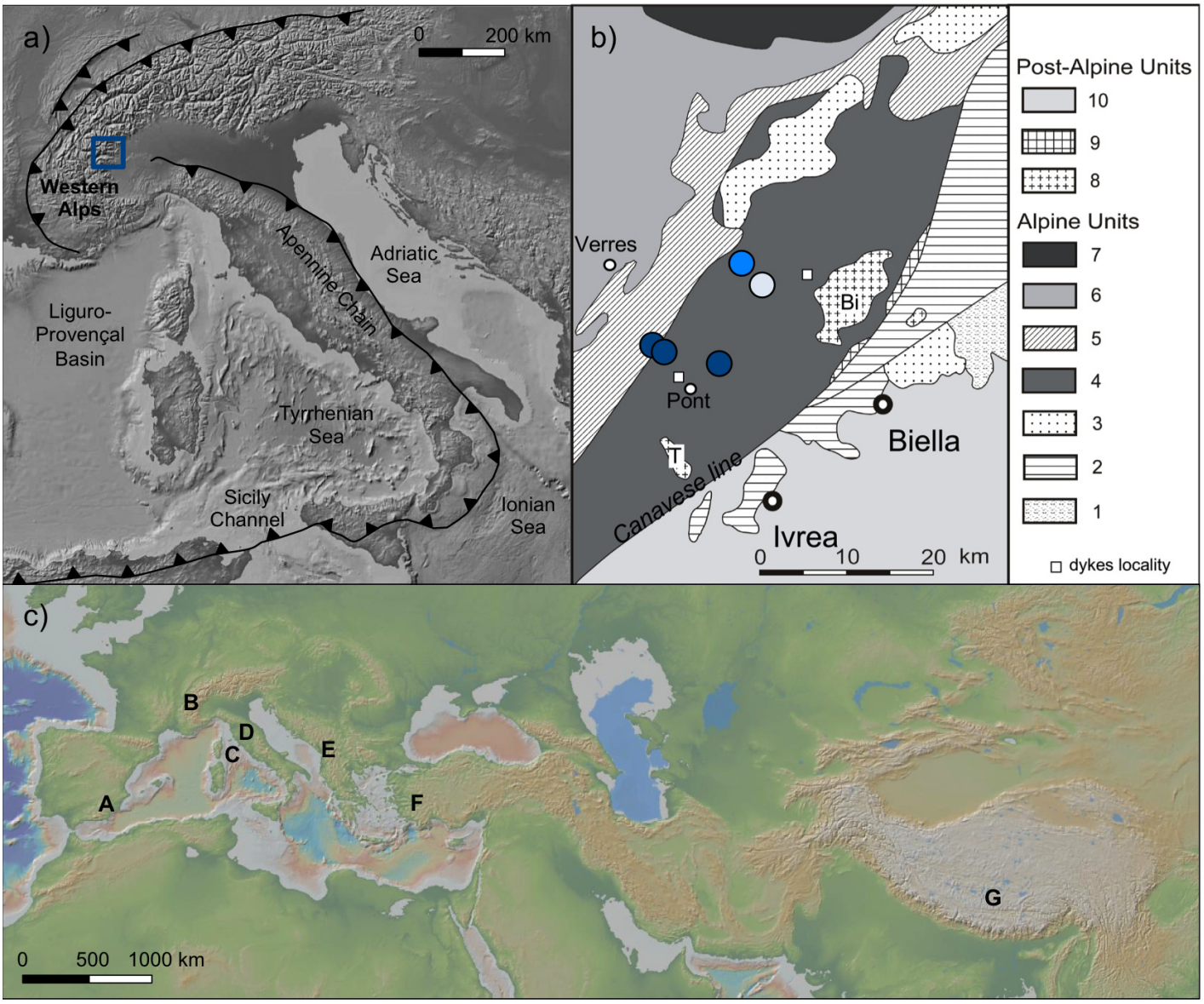

Fig. 1 - Distribution of the ultrapotassic and related magmatic products in the Western Alps highlighted in blue (modified after Del Piaz *et alii*, 1979, 1988; Del Piaz, 1992; Bistacchi *et alii*, 2001; Conticelli *et alii*, 2009 and Lepore *et alii*, 2017). a) Sketch map of the Italian peninsula region with major tectonic features; the study area is highlighted in blue; b) Western Alps Oligocene magmatism (modified after Conticelli *et alii*, 2009): 1- low grade Permian granite and granodiorite; 2- Ivrea zone mafic complex; 3- Ivrea zone kinzigitic rocks; 4- internal Sesia-Lanzo zone (eclogitic micashists); 5- external Sesia-Lanzo zone (gneiss complex); 6- Schistes Lustres and ophiolitic complex; 7- Monte Rosa and Gran Paradiso nappe (orthogneiss); 8- Oligocene Plutonic rocks, Traversella (T) and Biella plutons (Bi); 9- Oligocene volcanoclastic cover series; 10- Pleistocene-Holocene covers; selected samples are also reported: LMP are represented by dark blue circles, SHO and HKCA by light blue and pale blue, respectively; c) Shaded relief image of the Tethyan realm orogenic belts from Spain to Southern Tibet, showing the main outcropping areas of the Tethyan realm lamproites from west to east: (A) Murcia-Almeria, Spain; (B) Western Alps, Italy; (C) Corsica, France; (D) Tuscany, Italy; (E) Vardar Zone, Serbia and Macedonia; (F) Western Anatolia, Turkey; (G) West Lhasa Terrane, China.

Dal Piaz *et alii*, 1972, 1973, 1979, 1988; Venturelli *et alii*, 1984; Dal Piaz & Venturelli, 1985; Peccerillo & Martinotti, 2006; Owen, 2008; Conticelli *et alii*, 2009, 2010).

Lamproite and ultrapotassic rocks represent an interesting case-study for investigating the behaviour of Molybdenum and Uranium isotopes ($^{98}Mo/^{95}Mo$ and $^{238}U/^{235}U$) in subduction related rocks from mantle source enriched by extremely high proportion of a sedimentary recycled component. Recently, these non-traditional isotopic systematics emerged as important tools to reconstruct the paleo-redox conditions of the ocean and they have been proved to be promising diagnostic tracers of surface material recycled to the Earth's interior and back to the surface by volcanism (e.g., Kendall *et alii*, 2017; Willbold & Elliott, 2017; Freymuth *et alii*, 2015, 2016; Andersen *et alii*, 2014, 2015, 2017).

In this study the first data based on sediment-dominated, subduction-related magmas are reported and discussed in the frame of the definition of the role of sediment-melts in the metasomatism of the upper mantle. The data herewith reported are also the first $^{98}Mo/^{95}Mo$ and $^{238}U/^{235}U$ data ever performed on Italian volcanic rocks.

NON TRADITIONAL ISOTOPIC SYSTEMATICS

Molybdenum and Uranium are redox-sensitive trace elements with long ocean residence times (about 440 ky and 400 ky, respectively; Andersen *et alii*, 2017; Kendall *et alii*, 2017) and with similar redox behaviour in the ocean. They have generally low crustal concentrations (Mo ~1 ppm, U ~1.1 ppm bulk values; Taylor & Mclennan, 1985; Mclennan, 2001), and are among the most conservative trace elements in seawater (~10 ppb and ~3 ppb; Collier, 1985; Tissot & Dauphas, 2015). In oxic conditions, the only important sink for Mo and U in the oceans is Fe-Mn-crusts, while pelagic sediments represent only a minor sink (Andersen *et alii*, 2017; Kendall *et alii*, 2017). In reducing conditions U and particularly Mo are quantitatively removed from the water into anoxic sediment and into sediments at continental shelfs that become anoxic with depth (Andersen *et alii*, 2017; Kendall *et alii*, 2017.

Therefore, under oxidising conditions they assume conservative behaviour in the seawater whereas they are removed from the water columns and become enriched in the sediments under suboxic to anoxic conditions (i.e., continental margins; McManus *et alii*, 2006; Tribovillard *et alii*, 2012; Kendall *et alii*, 2017). This redox-sensitivity is the cause of significant mass-dependent isotope fractionation compared to seawater values, which has been used for constraining paleo-redox oceanic conditions (e.g., Andersen *et alii*, 2017; Kendall *et alii*, 2017 for review).

In oxic conditions Mo isotopes are strongly fractionated due to the incorporation of isotopically light Mo in Fe-Mn oxides (average $\delta^{98/95}$Mo about -1.00‰, Barling *et alii*, 2001; Siebert *et alii*, 2003) leaving seawater with a heavy isotope composition ($\delta^{98/95}$Mo ~ 2.09‰, Siebert *et alii*, 2003). In strongly reducing conditions Mo is quantitatively removed for the water column, without any isotopic fractionation, into anoxic sediments, which represent the major sink for Mo and provide a source of isotopically heavy Mo ($\delta^{98/95}$Mo from ~1.00‰ to 2.09‰, e.g., Kendall *et alii*, 2017). Suboxic sediments fill the gap between the two major sinks, displaying variable isotope composition (Kendall *et alii*, 2017).

Compared to Mo, U displays only minor isotope fractionation under oxic conditions (Algeo & Tribovillard, 2009; Noordmann *et alii*, 2015). Isotopically light U is adsorbed into Fe-Mn oxides (average $\delta^{238/235}$U of -0.59‰, Weyer *et alii*, 2008), whereas biogenic carbonates incorporate the seawater signature of -0.41‰ (Stirling *et alii*, 2007; Weyer *et alii,* 2008; Brennecka *et alii*, 2011; Romaniello *et alii*, 2013).

Under low-oxygen conditions, U is removed from seawater within suboxic and anoxic sediments, leading to deviations of the ^{238}U/^{235}U ratios and U concentrations relative to oxic environments (Weyer *et alii*, 2008; Montoya-Pino *et alii*, 2010; Brennecka *et alii*, 2011; Romaniello *et alii*, 2013). In these conditions the increase of reduced U-flux to anoxic facies (e.g., black shales) induces preferential removal of ^{238}U from seawater, resulting in relatively heavy isotope compositions. The $\delta^{238/235}$U values for suboxic sediments span between the seawater value and can reach values up to 0.43‰ in anoxic conditions (Weyer *et alii*, 2008).

Despite a substantial homogeneity of the bulk earth, significant variability exists at least between the isotope compositions of the upper mantle and the crust (i.e., MORBs: $\delta^{98/95}$Mo = -0.21‰ and $\delta^{238/235}$U = -0.26‰, average values from Willbold & Elliott, 2017; Andersen *et alii*, 2017; Crust: $\delta^{98/95}$Mo = 0.15‰ and $\delta^{238/235}$U = -0.29‰, average values from Tissot & Dauphas, 2016; Willbold & Elliott, 2017).

Uranium is a highly incompatible element and large isotope fractionations of U during either partial melting of the mantle or melting and/or dehydration of subducted material are considered to be unlikely (Andersen *et alii*, 2017). Thus, the deviation of U isotope composition of magmas from the typical mantle values is likely due to the addition of metasomatising components with distinct isotope signatures inherited directly from those of the subducted materials (i.e., AOC or sediments; Andersen *et alii*, 2017; Avanzinelli *et alii*, 2018). Melts from the sedimentary component show high Th/U and variably heavy $\delta^{238/235}$U (Andersen *et alii*, 2015; Avanzinelli *et alii*, 2018), whereas fluid from the altered mafic oceanic crust (AOC) have low Th/U and isotopically light $\delta^{238/235}$U (Andersen *et alii*, 2015, 2017).

Molybdenum is a moderately refractory siderophile/chalcophile element, highly incompatible in most magmatic phases (i.e., silicate; Willbold & Elliott, 2017) especially in presence of fluids at mantle condition (e.g., subduction zone, Bali *et alii*, 2012). Also, isotope fractionation of Mo during fractional crystallisation of typical magmatic phases should be very limited (Bezard *et alii*, 2016; Willbold & Elliott, 2017). On the other hand, Mo is compatible in mineralogical phases with elevated solid-melt partition coefficient such as sulphides and rutile ($D_{\text{Sulfidic melt/silicate melt}} < 20$ and $D_{\text{Rt/melt}} = 4$; Li & Audétat, 2012; Skora *et alii*, 2017). Although sulphide fractionation can potentially influence the Mo isotope composition of evolving magmatic systems, sulphur is only a minor component in silicate melts (<1% modal fractionation abundance), and it should not have a large effect on the Mo budget (Willbold & Elliott, 2017).

Molybdenum can also be fractionated during the dehydration or melting of the subducting slab due to its strong compatibility in rutile, both in equilibrium with a fluid ($D_{\text{fluid/Rt}} = 0.04$, Bali *et alii*, 2012) or with a magmatic melt (and $D_{\text{Rt/melt}} = 4$, Skora *et alii*, 2017). The available studies suggest that rutile preferentially incorporates light Mo isotopes: therefore slab-derived fluids and melts, generated in presence of residual rutile, should attain an isotopically heavy Mo signature, which is reflected in the high $\delta^{98/95}$Mo observed in most arc-related rocks (Willbold & Elliott, 2017).

On the other hand, the considerable amounts of Mo and U that are carried with the subducted components may preserve the originally variable isotopic composition of the subducted sediments and altered oceanic crust, hence imparting a characteristic isotope signature to the erupted magmas (e.g., Freymuth *et alii*, 2015, 2016).

In this complex scenario, according to the few data available, volcanic arcs dominated by AOC-derived fluids, show a substantially heavy Mo isotope composition, while those dominated by sediment-derived melts present a more variable isotope signature, which is generally light (Freymuth *et alii*, 2015), but can reach substantially heavier values when anoxic sediments are involved (Freymuth *et alii*, 2016).

PETROLOGICAL BACKGROUND AND SAMPLE SELECTION

The ultrapotassic rocks from the Western Alps represent the westernmost occurrence, together with Murcia-

Almeria ones (Spain), of the Tethyan Realm Lamproites (Tommasini *et alii*, 2011), which consist in a limited number small-volume of hypo-abyssal and volcanic rocks, with orogenic signature and lamproitic affinity, occurring as scattered outcrops from the Mediterranean area to south Tibet, along the orogenic belt related to the closure of the Tethyan ocean (Fig. 1c).

These magmatic rocks are the consequence of the late Tertiary (late Cretaceous) to Oligocene 'Alpine' subduction of the European plate beneath the Adriatic promontory that generated a belt of metasomatic mantle along the northern border of the African plate. Contemporary or after the subduction, this metasomatic mantle underwent partial melting at different times and in different zones in response to local modification of tectonics and thermal regimes (Peccerillo & Martinotti, 2006; Beltrando *et alii*, 2010). The collision was accommodated by crustal imbrications and subduction of continental material, as attested by the presence of UHP rocks in the Dora Maira massif (e.g., Chopin *et alii*, 1991; Gebauer *et alii*, 1997; Chopin & Schertl, 1999; Ferrando *et alii*, 2009). The western termination of the Alpine belt is a tight arc formed during the late Tertiary without any back-arc extension (Faccenna *et alii*, 2001; Mattei *et alii*, 2004).

The Western Alps are the site of post-collisional (i.e., Oligocene) ultrapotassic igneous activity that occurs within the restricted area of the Sesia-Lanzo north of the Canavese Line, but is absent in the Central and Eastern Alps (Fig. 1b). The sample selection includes three lamproites (VDA 17, VDA 2 and VDA 3, minettes), one shoshonite (VDA 14) and one sample belonging to the high-K calc-alkaline series (VDA 8, basaltic andesite). The ages of these products are all between 33 and 29 Ma (Dal Piaz *et alii*, 1972, 1973, 1979, 1988; Venturelli *et alii*, 1984; Dal Piaz & Venturelli, 1985), coeval with the peak of post-collisional magmatism of the entire Alps (34-30 Ma, Von Blanckenburg *et alii*, 1998).

Major, trace elements and radiogenic isotopes of these samples are reported in Table 1 (mostly from Conticelli *et alii*, 2009). For the sample VDA 2, Rare Earth Elements (hereafter REE) and Sr, Nd and Pb isotopes were specifically measured in order to complete the data set. The samples selected for the present study encompass the geochemical variations of the whole the magmatic province (Fig. 2).

The ultrapotassic rocks of this area have a lamproitic affinity considering that they are plagioclase-free micaceous dykes (minette) characterized by intersertal texture with phlogopite, clinopyroxene and K-feldspar, accompanied by minor olivine and riebeckite-arfvedsonite amphibole with accessory apatite, sphene and Fe-Ti oxides (Owen, 2008; Conticelli *et alii*, 2010). Shoshonitic to high-K calc-alkaline plagioclase-bearing lamprophyric rocks (kersantite to spessartite) are found associated in space and time with ultrapotassic rocks (Owen, 2008; Conticelli *et alii*, 2010).

These rocks, as well as all the Tethyan Realm Lamproites, can clearly be distinguished from other worldwide within-plate lamproites on the basis of their clear subduction-related signature (i.e., crust-like trace element-pattern and HFSE depletion; Fig. 2), as well as their radiogenic Sr-Pb and unradiogenic Nd isotope composition (Tommasini *et alii*, 2011).

The studied rocks are characterised by high MgO contents, indicating a primitive character, and variable K_2O and alkali contents, which define their serial affinity (Conticelli *et alii*, 2009).

TABLE 1

Major and trace elements composition along with radiogenic isotope compositions of Western Alps potassic and ultrapotassic magmatic rocks.

Unit:	*Rio Rechantez*	*Donnaz, Plan d'Albard*		*Cora Road*	*Niel*
Series:	LMP	LMP	LMP	SHO	HKCA
Sample:	**VDA 17**	**VDA 02**	**VDA 03**	**VDA 14**	**VDA 08**
Age (Ma)	30	30	30	30	30
SiO_2	52.15	57.75	57.50	54.24	55.44
TiO_2	1.20	1.32	1.37	0.97	1.00
Al_2O_3	10.62	10.73	10.64	14.43	17.60
Fe_2O_3	7.21	5.29	4.88	7.53	7.75
FeO	-	-	-	-	-
MnO	0.13	0.09	0.08	0.13	0.15
MgO	11.95	9.09	9.33	7.59	4.63
CaO	6.89	4.22	4.19	7.69	8.27
Na_2O	0.88	1.21	1.18	2.57	2.89
K_2O	7.66	9.23	9.64	3.90	1.86
P_2O_5	1.32	1.07	1.18	0.96	0.42
LOI	2.75	1.75	3.53	3.24	2.47
#Mg	79	80	82	70	58
Li	41	-	93	21	-
Sc	25	16	13	27	23
V	155	85	83	182	177
Cr	640	414	470	310	80
Co	33	27	25	26	16
Ni	300	298	280	140	40
Cu	60	58	30	50	< 10
Zn	80	99	90	90	90
Ga	17	18	19	19	20
Rb	395	546	555	172	63
Sr	829	815	799	882	560
Y	32	24	31	29	28
Zr	593	673	665	334	167
Nb	34	35	34	24	14
Cs	17	-	28	6	1
Ba	4293	3116	3797	2592	1046
La	117	103	106	56	41
Ce	273	237	260	127	78
Pr	38	39	37	17	9
Nd	174	164	169	75	35
Sm	34	36	34	16	7
Eu	6	7	6	3	2
Gd	19	23	19	10	6
Tb	2.0	2.5	1.9	1.3	0.9
Dy	8	8	7	6	5
Ho	1.2	1.1	1.2	1.0	0.9
Er	2.9	3.5	2.8	2.9	2.7
Tm	0.4	0.3	0.3	0.4	0.4
Yb	2,0	2.0	1.9	2.5	2.6
Lu	0.3	0.3	0.3	0.4	0.4
Hf	16	21	18	9	4
Ta	2.4	7.1	2.7	1.7	1.0
Pb	36	23	105	36	20
Th	155	164	134	72	20
U	28	31	22	22	5
$^{87}Sr/^{86}Sr_m$	0.71818	0.71796	0.71802	0.71241	0.71140
$^{87}Sr/^{86}Sr_i$	0.71759	0.71713	0.71717	0.71217	0.71126
$^{143}Nd/^{144}Nd_m$	0.51201	0.51204	0.51203	0.51213	0.51227
$^{143}Nd/^{144}Nd_i$	0.51199	0.51201	0.51200	0.51210	0.51224
$^{206}Pb/^{204}Pb_m$	18.878	18.704	18.690	18.847	18.727
$^{207}Pb/^{204}Pb_m$	15.718	15.689	15.717	15.681	15.671
$^{208}Pb/^{204}Pb_m$	39.472	39.072	39.093	39.031	38.918

Major and minor element contents are from Conticelli *et alii* (2009). Sr, Nd and Pb isotope compositions are from Conticelli *et alii* (2009) with the exception of VDA 2 sample that has been measured at the Radiogenic Isotopes Laboratory of the University of Firenze with a Thermo Finnigan Triton Thermal Ionisation Mass Spectrometer (TIMS). Mass bias was corrected by replicate analyses of NIST SRM 987, NIST SRM 981 and an internal reference material (NdFi) as described in Avanzinelli *et alii* (2005).

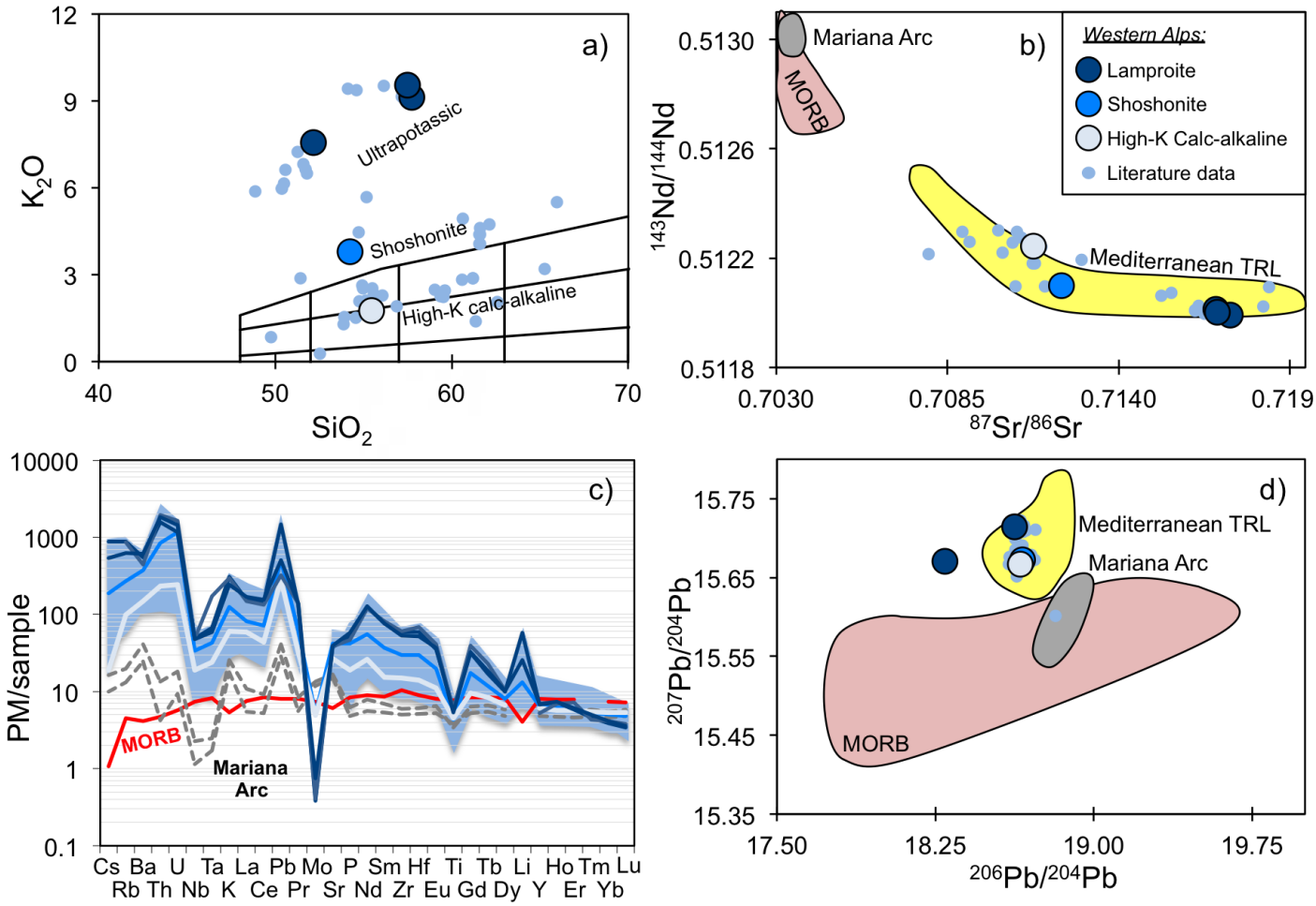

Fig. 2 - Geochemical and isotopic characteristics of Western Alps samples; a) K_2O vs. SiO_2 classification for orogenic volcanic rock suites (Peccerillo & Taylor, 1976); b) $^{87}Sr/^{86}Sr$ vs. $^{143}Nd/^{144}Nd$ and d) $^{206}Pb/^{204}Pb$ vs. $^{207}Pb/^{204}Pb$ isotope compositions of the studied samples compared to data from the literature (Venturelli *et alii*, 1984; Callegari *et alii*, 2004; Peccerillo & Martinotti, 2006; Owen, 2008; Prelević *et alii*, 2008; Conticelli *et alii*, 2009). Fields representing the wider range of Mediterranean Tethyan Realm Lamproite (Tommasini *et alii*, 2011) and the Mariana arc data (Elliott *et alii,* 1997) are also reported; c) Incompatible trace element patterns for mafic volcanic rocks normalised to the primordial mantle values (Sun & McDonough, 1989); MORB (grey line) from Gale *et alii* (2013), Mariana arc fluid- and sediment-dominated end-members (Guguan and Uracas, respectively; from Elliott *et alii,* 1997), are shown as representative of typical arc magmas.

Both the trace element and the isotope compositions clearly point to a significantly strong contribution of upper crustal component (i.e., sediments) in the mantle source of these rocks (Peccerillo & Martinotti, 2006; Conticelli *et alii*, 2007, 2009; Owen, 2008; Prelević *et alii*, 2008).

The incompatible trace element contents are generally high and positively correlated with K_2O (see Conticelli *et alii*, 2009). Lamproites have the highest levels of incompatible trace elements, including REE, and characteristic fractionation of LILE with respect to HFSE (Fig. 2c). Incompatible trace elements abundances generally decrease from ultrapotassic to high-K calc-alkaline mafic rocks, through shoshonites (Alagna *et alii*, 2010; Conticelli *et alii*, 2010). Significant troughs at Ta, Nb, and Ti with peaks at Th, U and Pb produce a typical orogenic-related sediment-dominated pattern for all the rock types, whereas a negative anomaly in Ba characterises only the ultrapotassic products (Conticelli *et alii*, 2009), similarly to other ultrapotassic Italian ultrapotassic products (Avanzinelli *et alii,* 2008).

The ultrapotassic rocks are also characterised by the highest $^{87}Sr/^{86}Sr$ and lowest $^{143}Nd/^{144}Nd$ values among Italian potassic to ultrapotassic magmas (Fig. 2b, Conticelli *et alii*, 2009, 2010), while calc-alkaline and shoshonitic terms fill the gap between upper crust and typical mantle values with lower $^{87}Sr/^{86}Sr$ and higher $^{143}Nd/^{144}Nd$. The crustal affinity of the ultrapotassic rocks is also confirmed by radiogenic Pb ratios despite their variability within the province is less evident than Sr and Nd isotopes (Fig. 2d).

ANALYTICAL METHODS

The determination of Mo and U contents and isotope compositions was performed using double spike techniques (^{97}Mo-^{100}Mo and ^{233}U-^{236}U, respectively) allowing both to correct the isotope ratios for instrumental mass bias and to calculate the concentration of U and Mo by isotope dilution. The protocols for sample dissolution and chemical purification are the same of Willbold *et alii* (2016) for Mo and Andersen *et alii* (2013, 2015) for

U. Measurements have been performed at the School of Earth Science of Bristol University with a ThermoFisher Neptune MC-ICP-MS. Repeated analyses of reference standard materials yielded $\delta^{98/95}$Mo = 0.043 ± 0.010‰ and [Mo] = 0.897 ± 0.023 ppm (n=8) for JB-2 reference standard (in agreement with Willbold *et alii*, 2016) and $\delta^{238/235}$U = -0.045 ± 0.037‰ and [U] = 5.82 ± 0.22 ppm (n= 8) for CZ-1 in-house standard uraninite and $\delta^{238/235}$U = -0.313 ± 0.076‰ and [U] = 0.157 ± 0.001 ppm (n= 3) for JB-2; the uncertainties cited represent 2σ standard deviations of repeat measurements of the same standard, hence representing the reproducibility of the analytical procedure. A replicate on two different powder aliquots of the same sample (VDA 14, Tab. 2) was also performed yielding Mo contents and isotope compositions identical within the reproducibility established from the standard.

Mo and U isotope composition are reported as the part per thousand deviation (δ-notation) of the ^{98}Mo/^{95}Mo and ^{238}U/^{235}U ratios relative to the NIST 3134 and the CRM 145 standards, respectively. Procedural blanks were <200 pg for Mo and <30 pg for U, thus negligible comparing with sample size (150 ng for Mo and 50 ng for U, respectively). Both Mo and U have been analysed in low-resolution mode, monitoring possible interfering elements along with the masses of interest. Mo masses were measured with 10^{11} Ω resistors, while for U a combination of 10^{10} Ω, 10^{11} Ω and 10^{12} Ω resistors were used to accommodate the presence of large (^{238}U), intermediate (^{235}U) and small (^{234}U) ion beams within the same configuration.

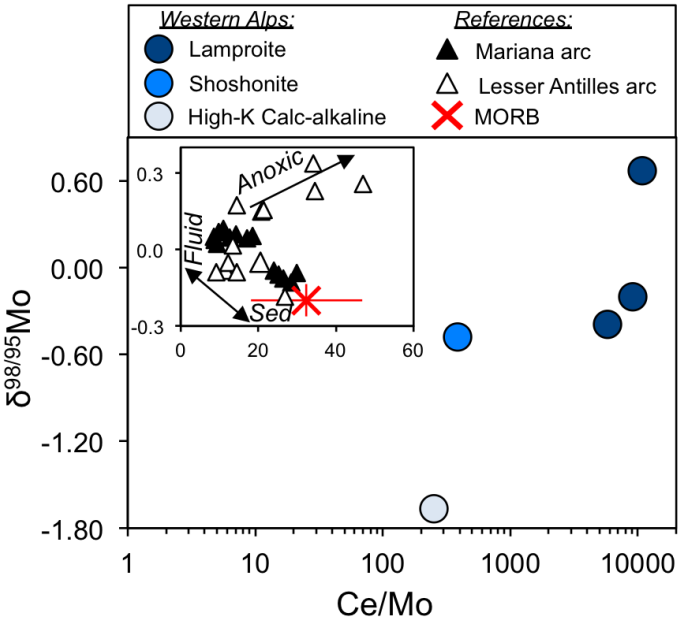

Fig. 3 - Mo isotope composition $\delta^{98/95}$Mo vs. Ce/Mo (log-scale) of Western Alps samples in comparison with Mariana arc and Lesser Antilles lavas (Freymuth *et alii*, 2015; 2016). MORB average is represented by the red symbol, with Ce/Mo from the compilation of Gale *et alii* (2013) and $\delta^{98/95}$Mo from Freymuth *et alii* (2015) (error bars are 2σ values). Error bars are smaller than the size of the symbols.

RESULTS

Molybdenum isotopes and concentrations

The analysed samples show significantly variable Mo isotopic composition with a total fractionation of about ~2‰ from the lightest sample ($\delta^{98/95}$Mo of -1.67‰, VDA 8) to the heaviest one ($\delta^{98/95}$Mo of 0.67 ‰, VDA 3)(Fig. 3, Tab. 2). The ubiquitously extremely low Mo content revealed by isotope dilution technique seems to correlate with K_2O, with the ultrapotassic samples having the lowest Mo contents (despite being the most enriched in other incompatible trace elements) along with the heaviest

TABLE 2

Molybdenum and Uranium isotope composition of Western Alps potassic and ultrapotassic magmas.

Series	Sample	δ98Mo NIST ‰	2 s.e.	ID Mo ppm	2 s.e.	δ238U ‰	2 s.e.	(234/238)	ID U ppm	2 s.e.
Western Alps										
LMP	**VDA 17**	-0.39	± 0.02	0.0473	± 0.0006	-0.25	± 0.03	0.980	30.29	± 0.10
LMP	**VDA 02**	-0.20	± 0.02	0.0258	± 0.0004	-0.28	± 0.04	0.963	34.41	± 0.12
LMP	**VDA 03**	0.67	± 0.09	0.0240	± 0.0050	-0.24	± 0.05	0.964	24.45	± 0.08
SHO	**VDA 14**	-0.48	± 0.03	0.336	± 0.004	-0.29	± 0.03	1.002	24.55	± 0.09
	rep	*-0.48*	*± 0.03*	*0.323*	*± 0.003*					
HKCA	**VDA 08**	-1.67	± 0.03	0.310	± 0.003	-0.30	± 0.02	1.004	5.05	± 0.02

	Sample	δ98Mo NIST ‰	2σ (n)	ID Mo ppm	2 s.e.	δ238U ‰	2σ (n)	(234/238)	ID U ppm	2 s.e.
RSMs										
	CZ-1	-	-	-		-0.045	± 0.037 (8)		5.82	± 0.22
	JB-2	0.043	± 0.010 (8)	0.890	± 0.023	-0.313	± 0.076 (3)		0.157	± 0.001

^{98}Mo/^{95}Mo and ^{238}U/^{235}U were measured via MC-ICPMS at BIG according to the procedure described in Willbold *et alii* (2016) and Andersen *et alii* (2013, 2015), respectively. The ^{97}Mo-^{100}Mo and IRMM-3636 ^{233}U-^{236}U double spike solutions have been used. The $\delta^{98/95}$Mo and $\delta^{238/235}$U were normalised to the International standard values measured along with the samples (NIST 3134 and CRM 145, respectively). The possible influence of secondary weathering was checked by measuring the (^{234}U/^{238}U) of the samples; parentheses denote isotope ratios are expressed as activity. Replicates (*rep*) are made on completely separate sample dissolutions. All errors are 2.s.e. and are fully propagated. Accuracy and reproducibility was tested over the measurement period by several replicates of Reference Standard Materials JB-2 and CZ-1 for which the reproducibility is expressed as 2σ; (n) = number of analyses

isotope composition (Mo content from 0.02 to 0.05 ppm, $\delta^{98/95}$Mo from 0.67 to -0.39‰). The isotopically heaviest sample (VDA 3) shows possible evidence of secondary alteration (i.e., high LOI value, Tab. 1), which may have affected both its Mo content and its isotope composition. Such a possibility will be discussed in more detail in the following section. The shoshonitic sample has Mo concentration one order of magnitude higher than the latter (0.33 ppm) and slightly lighter isotope composition ($\delta^{98/95}$Mo -0.48‰); the HKCA sample (VDA 8) has Mo content comparable to the shoshonite and the lightest $\delta^{98/95}$Mo of the province (-1.67‰). The low Mo content of ultrapotassic rocks is somehow surprising considering that Mo is an incompatible element in mantle-derived igneous rocks, which is inferred to behave similarly to Light-REE, according to the overall constancy of Ce/Mo ratio in terrestrial samples (Newsom *et alii*, 1986). In the studied samples this similarity is clearly not respected, as evident by the extremely high Ce/Mo of the studied rocks (especially the ultrapotassic ones, Fig. 3), hence requiring a process that removed most of the Mo. The absolute Mo content of high-K and shoshonitic samples is significantly lower than any typical arc lavas (e.g., the Mariana arc lavas: Elliott *et alii*, 1997; Freymuth *et alii*, 2015) and comparable just to the less Mo-abundant MORB (Gale *et alii*, 2013), both of which are otherwise orders of magnitude less enriched in incompatible trace elements (Fig. 2c). The Mo content of lamproitic rocks is extremely low, more than one order of magnitude lower than other studied samples.

Uranium isotopes and concentration

The analysed U isotope compositions are variable with a total range of <0.1‰. The ultrapotassic rocks show a narrow range of $\delta^{238/235}$U values (from -0.24 to -0.28‰) (Fig. 4, Tab. 2). The U concentrations calculated by isotopic dilution are well in agreement with those reported by previous studies (Conticelli *et alii*, 2009). Shoshonitic and high-K calc-alkaline samples have isotopically lighter $\delta^{238/235}$U values of -0.29‰ and -0.30‰, respectively. A slightly positive correlation between $\delta^{238/235}$U values and U content can be recognised: the more the ultrapotassic character, the higher U contents, the relatively heavier the isotope composition.

When (^{234}U/^{238}U) is considered (Figs. 5 and 6), only two out of five samples are within ±6‰ of secular equilibrium,

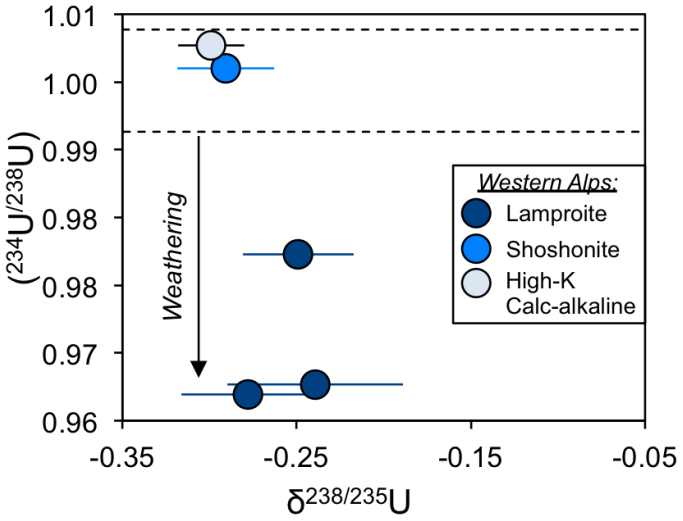

Fig. 5 - U isotope composition $\delta^{238/235}$U vs. (^{234}U/^{238}U) activity ratio. Only samples within ±6‰ of secular equilibrium were considered not affected by secondary alteration. Parentheses denote the ratio id expressed as activity.

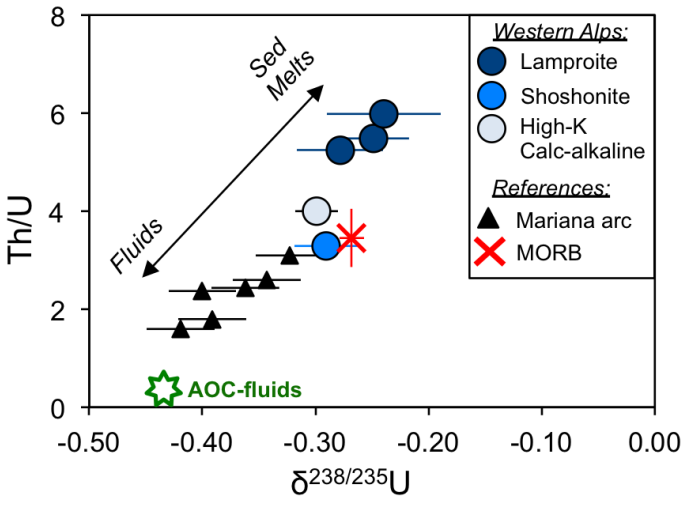

Fig. 4 - U isotope composition $\delta^{238/235}$U vs. Th/U for Western Alps samples in comparison with Mariana arc lavas (Andersen *et alii*, 2015; Elliott *et alii*, 1997). MORB and AOC (Altered Oceanic Crust) values are from Andersen *et alii* (2015).

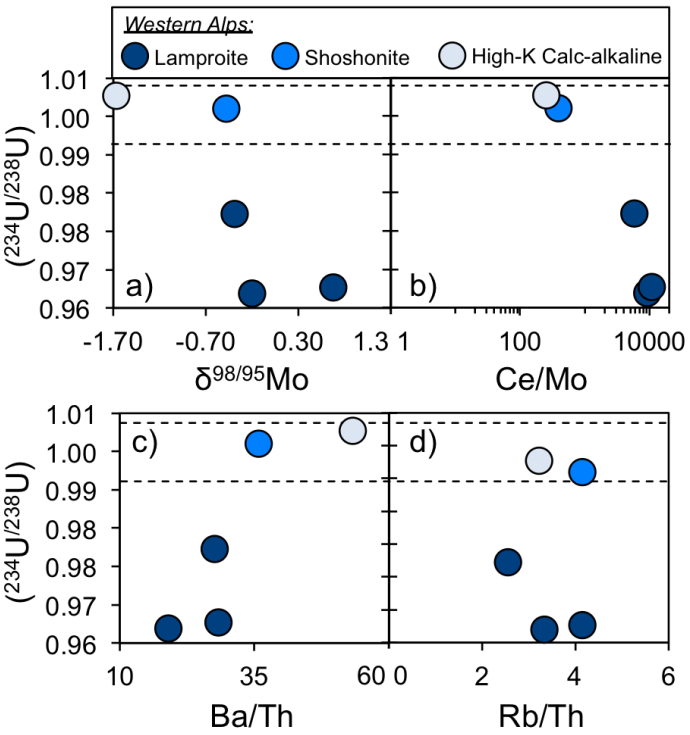

Fig. 6 - Various trace element ratios and $\delta^{98/95}$Mo vs. (^{234}U/^{238}U) activity ratio to investigate the role of superficial weathering. Parentheses denote the ratio id expressed as activity. Error bars for $\delta^{98/95}$Mo are smaller than the size of the symbols.

that is ($^{234}U/^{238}U$) = 1, entailing that these samples (mainly the ultrapotassic ones) must have experienced secondary alteration that preferentially removes ^{234}U over ^{238}U by leaching. However, the lack of correlation between $\delta^{238/235}U$ and ($^{234}U/^{238}U$) (Fig. 5) suggests that the weathering process, despite producing loss of ^{234}U, does not fractionate the $^{238}U/^{235}U$. This evidence is also strongly supported by the similar U isotope composition generally occurring in natural sample between the crust and rivers (Andersen *et alii*, 2017).

DISCUSSION

The origin of Mo depletion in ultrapotassic rocks

The samples of Western Alps lamproites show large U contents (up to 30 ppm) and extremely low Mo concentrations.

If U is considered as a proxy for recycled sedimentary material, then the negligible Mo contents required a process able to sequester or removed Mo either during the melting of the sedimentary material or later on, during melting of the veined metasomatic mantle, magma differentiation and/or possible secondary alteration.

The samples characterised by the lowest Mo content also have low ($^{234}U/^{238}U$), out of secular equilibrium, which is consistent with preferential removal of ^{234}U by superficial weathering. Such a process may have caused depletion of Mo as well (i.e., high Ce/Mo) (Fig. 6), due to the high mobility of Mo in fluids (Bali *et alii*, 2012). Taking the decrease of ($^{234}U/^{238}U$) as an index of weathering, we compare it to Ce/Mo as well as to other ratios between fluid-mobile elements (such as Ba, U and Rb) and the immobile Th (Fig. 6). A broad positive correlation is observed between ($^{234}U/^{238}U$) and Ba/Th (Fig. 6; and also U/Th, not shown) consistent with weathering-related depletion, but the same is not true for Rb/Th (Fig. 6) showing, if any, an opposite behaviour. In addition, the low Ba/Th is a common characteristic of many Italian ultrapotassic rocks that has been related to an original Ba depletion in the down-going sediments (Avanzinelli *et alii*, 2008). Furthermore, the magnitude of Mo depletion is more significant than that of Ba and U, implying that, if weathering is responsible for its extensive removal, it must have affected other fluid-mobile elements to a much lesser extent.

In terms of Mo isotope composition, the samples showing the heaviest $\delta^{98/95}Mo$ (VDA 2 = -0.20‰ and VDA 3= 0.67‰, respectively) seem also to be the more weathered having the lowest ($^{234}U/^{238}U$) (Fig. 6a). On the other hand, superficial weathering in oxidising conditions should preferentially remove the heavy ^{98}Mo with respect to the light ^{95}Mo, leaving the rocks with isotopically light $\delta^{98/95}Mo$. This sense of isotope fractionation is clearly demonstrated by ubiquitously heavy isotope composition of rivers ($\delta^{98/95}Mo$ = 0.7‰ on average, according to Archer & Vance, 2008). If the Mo depletion was due to such a process, we should have expected lower $\delta^{98/95}Mo$ for the most Mo-depleted rocks, which is the opposite to what is observed among the studied samples.

Alternative processes that may potentially be responsible for the extreme depletion of Mo from the magmas imply the presence of specific mineral phases, involved either during sediment melting or during magma genesis and differentiation, which are able to sequester consistent amount of Mo, such as rutile, sulphides and Fe-Mn crusts or nodules.

As outlined above, rutile should preferentially host light Mo (Freymuth *et alii* 2015; Skora *et alii*, 2017; Willbold & Elliott, 2017), thus both Mo depletion and heavier isotope composition of lamproites could reflect an increasing role for sediment melts with residual rutile. Such a process, however, should also produce a concomitant depletion in Nb from lamproites to high-K calc-alkaline products, which on the contrary is not observed (see Fig. 2c).

Porphyry Cu ± Mo ± Au deposits are the most characteristic sulphide-rich mineral deposits associated to subduction and collisional processes (Richards, 2015). In fact, the distribution of porphyry deposits along the Tethyan orogen is not uniform either in space or time, and they are particularly missing in the western Mediterranean area (i.e., Spain and Alps; Richards, 2015). Therefore, although the potential of sulphides to induce Mo isotope fractionation, it seems unlikely that the extremely low Mo contents in the erupted products could be linked to the occurrence of syn- or post-collisional forming porphyry deposits in the western Tethys. Anyway, a major role of sulphides at any stage of the magma genesis or differentiation should also result in a significant depletion of chalcophile elements such as Pb, Cu, and Ga. The ultrapotassic Mo-depleted samples display Ce/Pb comparable to global arcs, whilst Ce/Mo is almost two orders of magnitude greater, implying that the process that depletes Mo does not affect Pb (Fig. 7); the same holds true for Ga (not shown). Also, Pb is generally enriched in these rocks with respect to other incompatible trace elements, as evident from the primordial mantle normalised patterns (Fig. 2c).

Fe-Mn nodules can host large amount of Mo (up to 1000's ppm, Barling *et alii*, 2001; Hein *et alii*, 2003) and have extremely light isotope composition ($\delta^{98/95}Mo$ down to -1.49‰, Barling *et alii*, 2001). In principle, the residual presence of these nodules (which may host most of the subducted Mo) during sediment melting, or their removal from the sediment pile in the early phases of the subduction,

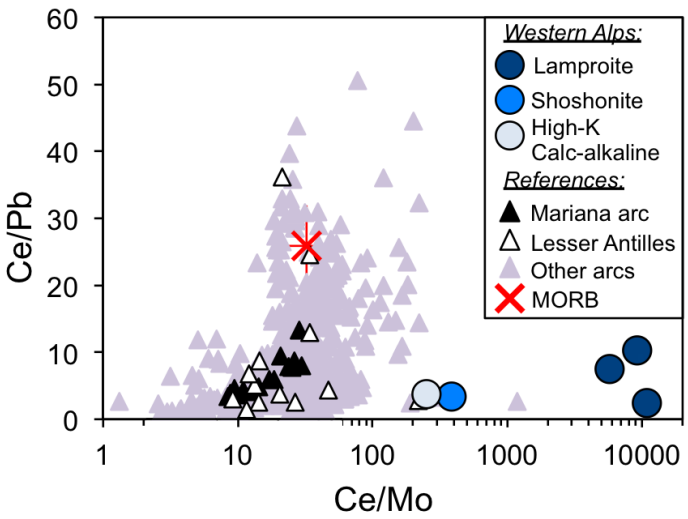

Fig. 7 - Ce/Mo (log-scale) vs. Ce/Pb trace element ratios reported to investigate the behaviour of Mo. Western Alps magmas are compared and Mariana arc lavas (Freymuth *et alii*, 2015; Elliott *et alii*, 1997) and other arcs from GeoRoc (georoc.mpch-mainz.gwdg.de/georoc/).

may explain both the Mo depletion and $\delta^{98/95}$Mo of the ultrapotassic Western Alps samples. However, this process would also deplete other elements that are enriched in the same nodules or crust, such as Pb and LREE (along with Mn and Tl), which are not anomalously depleted in the studied samples, as explained above.

It is also difficult to explain the depletion of Mo in the general framework of the genesis of ultrapotassic lamproitic rocks described in the introduction. The decrease of the enrichment of most of incompatible trace element contents, such as U, from ultrapotassic rocks to high-K calc-alkaline ones, is consistent with melting at progressively higher degrees of a veined mantle (Foley, 1992; Prelević *et alii*, 2008; Conticelli *et alii*, 2007, 2009, 2015). In this context, however, the depletion of Mo in the ultrapotassic lamproites could only be explained by the presence of a specific Mo-rich phase that remains residual during the melting of the phlogopite-rich metasomatic veins. Classic metasomatic phases, including K-rich micas, do not host significant amount of Mo (Adam & Green, 2006), and, in any case, their presence in the residue should result in a depletion of Rb, which is not observed in our lamproitic rocks. Other more particular metasomatic phases cannot be excluded, but no correlation with other geochemical indices has been found so far.

In summary, it was not possible to find a unique suitable process to account for the extreme depletion in Mo in the studied rocks, especially the ultrapotassic ones. It possible that some of the processes outlined above may variably contribute to produce such a feature, but further investigation is required.

Comparison with other subduction-related magmas

In this section the U and Mo isotope composition of the studied magmas is discussed in relationship to that of other subduction-related rocks, keeping in mind that some of the isotopic variability, especially for Mo, might have been affected by the not completely resolved processes responsible for the Mo depletion.

Globally, the geochemical and long-lived isotopic (Sr-Nd-Pb) composition of subduction-related volcanic rocks is governed by the variable contribution of three main components (e.g., Elliott, 2003) (Fig. 8): i) the depleted mantle (DM); ii) the slab-derived 'fluids', isotopically similar to the partially altered subducted basaltic oceanic crust (AOC); iii) the slab-derived 'melts', with isotope signatures suggesting its derivation from the subducted sediments.

As outlined above the Western Alps samples fall at high Th/Nb, together with sediment-melt dominated arc magmas (Elliott, 2003) and other Italian ultrapotassic rocks (Avanzinelli *et alii*, 2009), with Th/Nb decreasing from ultrapotassic to shoshonitic and high-K calc-alkaline rocks.

In terms of $\delta^{238/235}$U and $\delta^{98/95}$Mo, AOC-derived fluids are believed to be respectively light (Andersen *et alii*, 2015) and relatively heavy (Freymuth *et alii*, 2015; König *et alii*, 2016). The effect of sediment melt addition is more complex, especially for Mo isotopes. König *et alii* (2016) and Freymuth *et alii* (2015) reported lowering of $\delta^{98/95}$Mo values with increasing sediment-melt contribution. On the other hand, if anoxic sediments are involved (e.g., Lesser Antilles, Freymuth *et alii*, 2016) the sediment component is suggested to drive the composition of the magmas to heavy $\delta^{98/95}$Mo values.

In the case of $\delta^{238/235}$U the sediment component is generally believed to be similar to the Bulk Earth value (-0.30‰, Andersen *et alii*, 2015), although heavier compositions has been recently reported for carbonate-rich sediments (i.e., marls: Avanzinelli *et alii*, 2018).

In the $\delta^{238/235}$U vs. Th/U diagram (Fig. 4; Andersen *et alii*, 2015) the studied samples extend the general positive correlation displayed by the Marianas arc, with progressively increasing Th/U and heavier $\delta^{238/235}$U from the high-K calc-alkaline to the ultrapotassic terms. This is consistent with an increasing contribution of the sediment-derived component into the source of these magmas.

The picture is more complex when Mo isotopes are considered. The high-K calc-alkaline and shoshonitic samples have light $\delta^{98/95}$Mo, even lighter than those reported by Freymuth *et alii* (2015) and König *et alii* (2016) for sediment-dominated magmas. This is consistent with the addition of an isotopically light sediment-melt component,

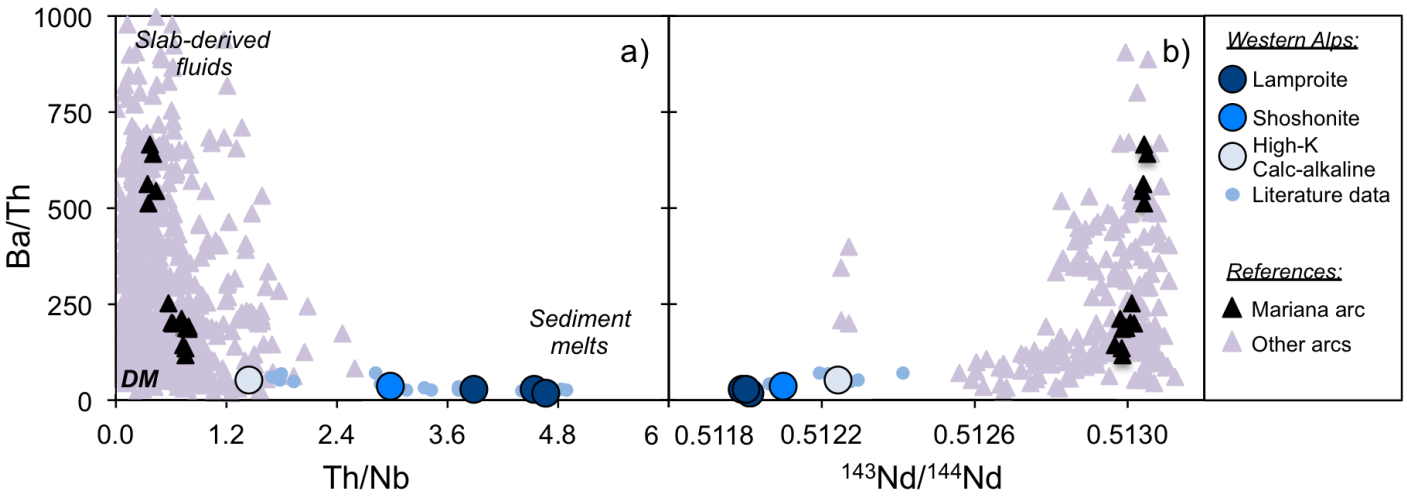

Fig. 8 - a) Th/Nb vs. Ba/Th; b) ^{143}Nd/^{144}Nd vs. Ba/Th of Western Alps ultrapotassic and related rocks. Mariana arc lavas are from Elliott *et alii* (1997) other arcs are from GeoRoc (georoc.mpch-mainz.gwdg.de/georoc/).

similar to what observed in other arcs (Freymuth *et alii*, 2015; König *et alii*, 2016), and in agreement with the sediment-dominated character of these magmas, where the contribution of subduction-related fluids is probably obscured by that of the sediment melt.

On the other hand, the ultrapotassic rocks do not fit this model, showing widely variable $\delta^{98/95}$Mo values, actually exceeding the whole range measured so far in subduction related magmas, spanning from light to heavy $\delta^{98/95}$Mo values. This may be somewhat related to the extreme depletion in absolute Mo content described above, hence requiring a process, not yet identified, capable of retaining Mo and also modifying its isotope composition.

The SALATHO component of the Tethyan Realm Lamproites

The studied samples belong the Tethyan Realm Lamproites, showing several peculiar characteristics with respect to typical arc magmas (Tommasini *et alii*, 2011), which can be discussed also in term of the $\delta^{238/235}$U and $\delta^{98/95}$Mo of the studied magmas.

Tommasini *et alii* (2011) pointed out that the Tethyan Realm lamproites and lamprophyres share a common positive correlation between Th/La and Sm/La ratios (Fig. 9a). Such positive correlation is apparently opposite to that observed in typical arc volcanic rocks (Plank, 2005) and it requires a peculiar reservoir with high Sm/La and extraordinary high Th/La ratios (i.e., SALATHO; Tommasini *et alii*, 2011). 'Ordinary' metasomatic agents are unable to reproduce a mantle source that would account for magmas with Th/La > 1, Sm/La > 0.3 and Th/U > 4 (Plank, 2005; Tommasini *et alii*, 2011; Conticelli *et alii*, 2011, 2015). The authors suggested that the SALATHO signature derived from the enrichment of the sub-continental lithospheric mantle with a further subduction-related ancient component (Tommasini *et alii*, 2011). Thus two distinct metasomatic events were inferred: i) an ancient one (older than few hundreds of million years) providing the SALATHO component, the origin of which is still uncertain, but was tentatively linked to the recycling of slivers of altered old oceanic crust at relatively low grade of metamorphism with re-mobilisation of lawsonite and epidote (featuring the high Sm/La and Th/La ratios); ii) a younger one derived from the partial melting of recycled sediments during subduction, producing the typical K_2O and related incompatible trace elements enrichments of ultrapotassic rocks from destructive plate margins (e.g., Conticelli *et alii*, 1992, 2009; Benito *et alii*, 1999; Turner *et alii*, 1999; Prelević *et alii*, 2008, 2010; Avanzinelli *et alii*, 2009; Tommasini *et alii*, 2011).

The studied samples show a clear contribution from the SALATHO component (Fig. 9). No correlation is observed between Th/La (as index of the SALATHO) and $\delta^{238/235}$U (Fig. 9c), suggesting that U is mainly controlled by the second metasomatic event related to sediment melting, in agreement with what discussed in the previous section. A broad increase of $\delta^{98/95}$Mo with Th/La is observable from high-K calc-alkaline to ultrapotassic terms, although the heaviest sample lies outside the trend (Fig 9b). This may suggest that the still uncertain processes that formed the SALATHO component were also responsible for widely variable $\delta^{98/95}$Mo and the strong depletion of Mo observed in the studied rocks.

CONCLUSIONS

The original U and Mo isotope data presented in this study are among the few presented for sediment-

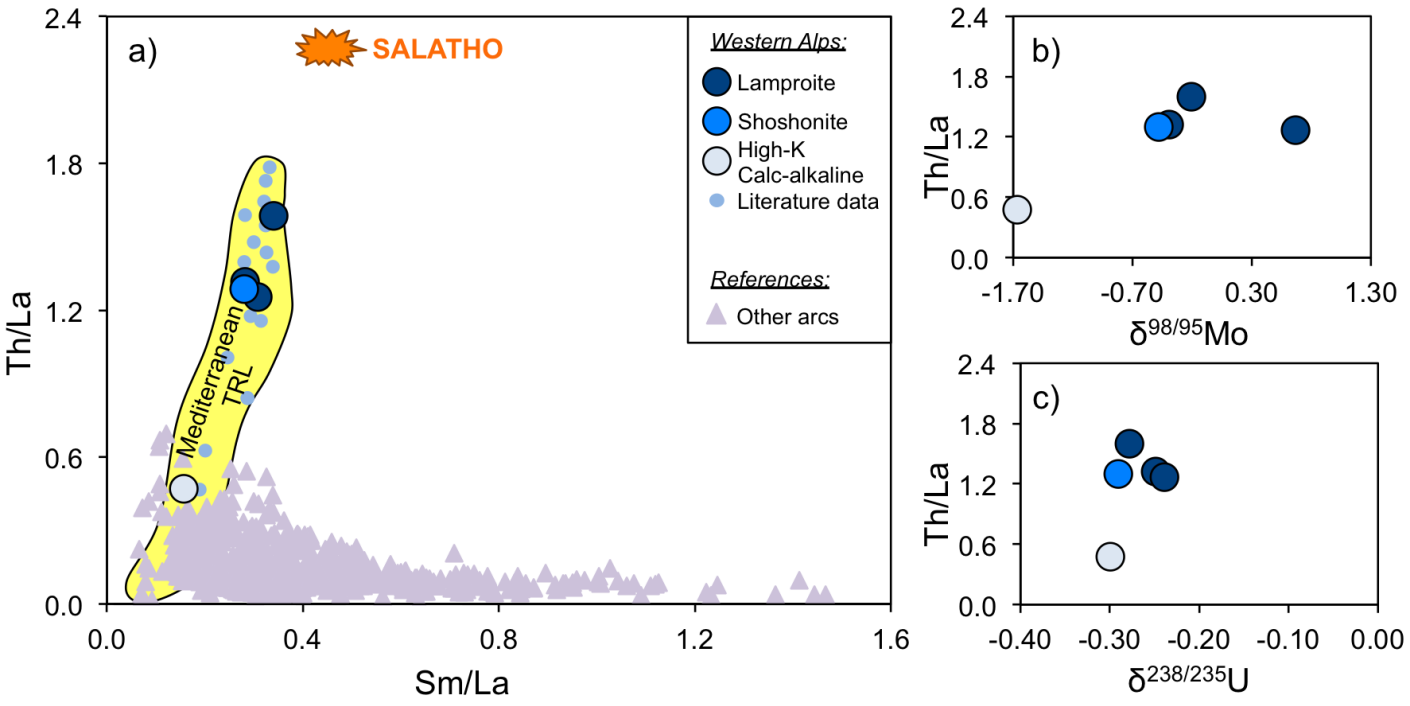

Fig. 9 - a) Sm/La vs. Th/La of the studied Italian ultrapotassic and related samples along with the Mediterranean TRL from Tommasini *et alii* (2011), and other subduction-related arcs from GeoRoc (georoc.mpch-mainz.gwdg.de/ georoc/); b) $\delta^{98/95}$Mo vs. Th/La; c) $\delta^{238/235}$U vs. Th/La.

dominated subduction-related magmatic rocks and are the first data published on Italian magmatism. Within the studied magmatic province a large variation in isotope compositions occurs, both for Mo and U isotopes. U isotope compositions are consistent with a dominant role for recycled sediment melts increasing along with the enrichment in K and incompatible trace elements.

The picture is more complex for Mo and its isotopes. Mo in Western Alps rocks is extremely depleted with respect to any other trace elements, including fluid-mobile ones (e.g., U or Ba), elements preferentially transferred by melts (e.g., Ce or Th) and chalcophile trace metals (e.g., Pb or Ga). $\delta^{98/95}$Mo is largely variable exceeding the variation observed in global arcs between fluid- and sediment-dominated arcs.

The geochemical and isotope composition of high-K calc-alkaline and shoshonitic rocks is again consistent with the addition of a subduction-derived sediment melt component with low $\delta^{98/95}$Mo and relatively high Ce/Mo. On the contrary, a different process is required to account for the extreme depletion of Mo of the ultrapotassic samples.

Such a process does not only affect Mo contents, but also may be related to significant isotope fractionation, producing the variably heavier $\delta^{98/95}$Mo of lamproites; thus to understand this conundrum is also fundamental to explain the observed Mo isotope variations. Several hypotheses have been tested to explain these features, including i) secondary weathering, testified by the low (^{234}U/^{238}U) of some of the studied samples, ii) removal of Mo-rich phases such as rutile, sulphides or Fe-Mn crust, and iii) the presence of specific residual phases during melting of the metasomatised mantle; iv) the complex and still unresolved processes responsible also for the genesis of the SALATHO component that affects all the Tethyan Realm Lamproites.

None of these processes can, by itself, explain the Mo systematics of the studied rocks, although future investigation on other orogenic ultrapotassic rocks with lamproitic affinity may help to shed some lights on this matter.

Acknowledgments

The author thanks Tim Elliott, for allowing access to Mo and U isotopic facilities of the BIG (Bristol Isotope Group) while at the Bristol University, Chris Coath, for technical support with Mass Spectrometry. A special thank to Sandro Conticelli for supplying the analysed samples, to Riccardo Avanzinelli for revising an earlier version of this manuscript, and to Heye Freymuth, Kate Hibbert, Remco Hin, Tim Elliott, and Simone Tommasini for sharing time and fruitful discussions during both the analytical and scientific work. Comments of Dr. Samuele Agostini and an Prof. Dejan Prelević helped improving this manuscript. Financial support was provided by a 'Pegaso' Doctoral Fellowship at the Universities of Florence and Pisa, and by PRIN 2010-2011 and 2015 both issued to Sandro Conticelli with grants 2010TT22SC_001 and 20158A9CBM, respectively.

REFERENCES

Adam J. & Green T. (2006) - *Trace element partitioning between mica- and amphibole-bearing garnet lherzolite and hydrous basanitic melt: 1. Experimental results and the investigation of controls on partitioning behavior.* Contrib. Mineral. Petr., **152**, 1-17.

Alagna K.E., Peccerillo A., Martin S. & Donati C. (2010) - *Tertiary to present evolution of orogenic magmatism in Italy*. J. Virtual Explorer, **36**, 1-63.

Algeo T.J. & Tribovillard N. (2009) - *Environmental analysis of paleoceanographic systems based on molybdenum-uranium covariation.* Chem. Geol., **268**, 211-225.

Altherr R., Meyer H.P., Holl A., Volker F., Alibert C. & McCulloch M.T., Majer V. (2004) - *Geochemical and Sr-Nd-Pb isotopic characteristics of late Cenozoic leucite lamproites form East European Alpine belt (Macedonia and Yugoslavia)*. Contrib. Mineral. Petr., **147**, 58-73.

Altherr R., Topuz G., Siebel W., Şen C., Meyer H.P., Satir M. & Lahaye Y. (2008) - *Geochemical and Sr-Nd-Pb isotopic characteristics of Paleocene plagioleucitites from the eastern Pontides (NE Turkey)*. Lithos, **105**, 149-161.

Andersen M.B., Elliott T., Freymuth H., Sims K.W.W., Niu Y. & Kelley K.A. (2015) - *The terrestrial uranium isotope cycle.* Nature, **517**, 356-359.

Andersen M.B., Romaniello S., Vance D., Little S.H., Herdman R. & Lyons T.W. (2014) - *A modern framework for the interpretation of $^{238}U/^{235}U$ in studies of ancient ocean redox*. Earth Planet. Sc. Lett., **400**, 184-194.

Andersen M.B., Stirling C.H. & Weyer S. (2017) - *Uranium isotope fractionation*. Rev. Mineral. Geochem. **82**(1), 799-850.

Andersen M.B., Vance D., Keech A.R., Rickli J., Hudson G. (2013) - *Estimating U fluxes in a high-latitude, boreal post-glacial setting using U-series isotopes in soils and rivers*. Chem. Geol., **354**, 22-32.

Archer C. & Vance D. (2008) - *The isotopic signature of the global riverine molybdenum flux and anoxia in the ancient oceans*. Nature Geosci., **1**, 597-600.

Avanzinelli R., Boari E., Conticelli S., Francalanci L., Guarnieri L., Perini G., Petrone C.M., Tommasini S. & Ulivi M. (2005) - *High precision Sr, Nd, and Pb isotopic analyses using the new generation thermal ionisation mass spectrometer thermofinnigan triton-Ti®.* Period. Mineral., **75**, 147-166.

Avanzinelli R., Casalini M., Elliott T. & Conticelli S. (2018) - *Carbon fluxes form subducted carbonates revealed by uranium excess at Mount Vesuvius, Italy.* Geology, **46**, 259-262.

Avanzinelli R., Elliott T., Tommasini S. & Conticelli S. (2008) - *Constraints on the genesis of potassium-rich Italian volcanic rocks from U/Th disequilibrium*. J. Petrol., **49**, 195-223.

Avanzinelli R., Lustrino M, Mattei M., Melluso L. & Conticelli S. (2009) - *Potassic and ultrapotassic magmatism in the circum-Tyrrhenian region: significance of carbonated pelitic vs. pelitic sediment recycling at destructive plate margin.* Lithos, **113**, 213-227.

Bali E., Keppler H. & Audetat A. (2012) - *The mobility of W and Mo in subduction zone fluids and the Mo-W-Th-U systematics of island arc magmas.* Earth Planet. Sc. Lett., **351-352**, 195-207.

Barling J., Arnold G. & Anbar A. (2001) - *Natural mass-dependent variations in the isotopic composition of molybdenum.* Earth Planet. Sc. Lett., **193**, 447-457.

Beltrando M., Lister G.S., Rosenbaum G., Richards S. & Forster M.A. (2010) - *Recognizing episodic lithospheric thinning along a convergent plate margin: The example of the Early Oligocene Alps*. Earth-Sci. Rev., **102**, 81-98.

Benito G.R., Lopez Ruiz J., Cebria J.M, Hertogen J., Doblas M., Oyarzun R. & Demaiffe D. (1999) - *Sr and O isotope constraints on source and crustal contamination in the High-K calc-alkaline and shoshonitic Neogen volcanic rocks of SE Spain*. Lithos, **46**, 773-802.

Bergman S.C. (1987) - *Lamproites and other potassium-rich igneous rocks: a review of their occurrence, mineralogy and geochemistry*. Geol. Soc. Sp., **30**, 104-190.

Bezard R., Fischer-Gödde M., Hamelin C., Brennecka G.A. & Kleine T. (2016) - *The effects of magmatic processes and crustal recycling on the molybdenum stable isotopic composition of Mid-Ocean Ridge Basalts* Earth Planet. Sc. Lett., **453**, 171-181.

Brennecka G.A., Herrmann A.D., Algeo T.J. & Anbar A.D. (2011) - *Rapid expansion of oceanic anoxia immediately before the end-Permian mass extinction*. P. Natl. Acad. Sci. USA, **108**, 17631-17634.

Bistacchi A., Dal Piaz G.V., Massironi M., Zattin M. & Balestrieri M.L. (2001) - *The Aosta-Ranzola extensional fault system and Oligocene-Present evolution of the Austroalpine-Penninic wedge in the north-western Alps*. Intern. J. Earth Sci., **90**, 654-667.

Callegari E., Cigolini C., Medeot O. & D'Antonio M. (2004) - *Petrogenesis of calc-alkaline and shoshonitic post-collisional Oligocene volcanics of the Cover Series of the Sesia Zone, Western Italian Alps*. Geodin. Acta, **17**, 1-29.

Carlson R.W. & Irving A.J. (1994) - *Depletion and enrichment history of subcontinental lithospheric mantle: an Os, Sr, Nd and Pb isotopic study of ultramafic xenoliths from the northwestern Wyoming Craton*. Earth Planet. Sc. Lett., **126**(4), 457-472.

Chopin C. & Schertl H.P. (1999) - *The UHP unit in the Dora-Maira massif, western Alps*. Int. Geol. Re., **41**, 765-780.

Chopin C., Henry C. & Michard A. (1991) - *Geology and petrology of the coesite-bearing terrain, Dora Maira massif, Western Alps*. Eur. J. Miner., **3**, 263-291.

Collier R.W. (1985) - *Molybdenum in the northeast Pacific Ocean*. Limnol. Oceanogr., **30**, 1351-1354.

Conticelli S. (1998) - *The effects of crustal contamination on ultrapotassic magmas with lamproitic affinity: mineralogical, geochemical and isotope data from the Torre Alfina lavas and xenoliths, Central Italy*. Chem. Geol., **149**, 51-81.

Conticelli S. & Peccerillo A. (1992) - *Petrology and geochemistry of potassic and ultrapotassic volcanism in Central Italy: petrogenesis and interferences on the mantle source*. Lithos, **28**, 221-240.

Conticelli S., Avanzinelli R., Ammannati E. & Casalini M. (2015) - *The role of carbon from recycled sediments in the origin of ultrapotassic igneous rocks in the Central Mediterranean*. Lithos, **232**, 174-196.

Conticelli S., Avanzinelli R., Marchionni S., Tommasini S. & Melluso L. (2011) - *Sr-Nd-Pb isotopes from the Radicofani Volcano, Central Italy: constraints on heterogeneities in a veined mantle responsible for the shift from ultrapotassic shoshonite to basaltic andesite magmas in a post-collisional setting*. Miner. Petrol., **103**, 123-148.

Conticelli S., Avanzinelli R., Poli G., Braschi E. & Giordano G. (2013) - *Shift from lamproite-like to leucititic rocks: Sr-Nd-Pb isotope data from the Monte Cimino volcanic complex vs. the Vico stratovolcano, Central Italy*. Chem. Geol., **353**, 246-266.

Conticelli S., Carlson R.W., Widom E. & Serri G. (2007) - *Chemical and isotopic composition (Os, Pb, Nd, and Sr) of Neogene to Quaternary calc-alkalic, shoshonitic, and ultrapotassic mafic rocks from the Italian peninsula: inferences on the nature of their mantle sources*. In: Beccaluva L., Bianchini G., Wilson M. (Eds.), *Cenozoic volcanism in the Mediterranean area*. Geol. S. Am. S., **418**, 171-202.

Conticelli S., D'Antonio M., Pinarelli L. & Civetta L. (2002) - *Source contamination and mantle heterogeneity in the genesis of Italian potassic and ultrapotassic volcanic rocks: Sr-Nd-Pb isotope data from Roman Province and Southern Tuscany*. Miner. Petrol., **74**, 189-222.

Conticelli S., Guarnieri L., Farinelli A., Mattei M., Avanzinelli R., Bianchini G., Boari E., Tommasini S., Tiepolo M., Prelévic D. & Venturelli G. (2009) - *Trace elements and Sr-Nd-Pb isotopes of K-rich to shoshonitic, and calc-alkalic magmatism of the Western Mediterranean region: Genesis of ultrapotassic to calc-alkaline magmatic associations in a post-collisional geodynamic setting*. Lithos, **107**, 68-92.

Conticelli S., Laurenzi M.A, Giordano G., Mattei M., Avanzinelli R., Melluso L., Tommasini S., Boari E., Cifelli F. & Perini G. (2010) - *Leucite-bearing (kamafugitic/leucititic) and -free (lamproitic) ultrapotassic rocks and associated shoshonites from Italy: constraints on petrogenesis and geodynamics*. In: Beltrando M., Peccerillo A., Mattei M., Conticelli S., Doglioni C. (Eds.), *The Geology of Italy*. J. Virtual Explorer, **36**, 1-95.

Conticelli S., Manetti P. & Menichetti S. (1992) - *Petrology, chemistry, mineralogy and Sr isotopic features of Pliocenic Orendites from South Tuscany: implications on their genesis and evolutions*. Eur. J. Mineral., **4**, 1359-1375.

Conticelli S., Melluso L., Perini G., Avanzinelli R. & Boari E. (2004) - *Petrologic, geochemical and isotopic characteristics of potassic and ultrapotassic magmatism in Central-Southern Italy: inferences on its genesis and on the nature of mantle sources*. Period. Mineral., **73**, 135-164.

Dal Piaz, G.V. (1992) - *Guide Geologiche Regionali, vol. 3, Le Alpi dal Monte Bianco al Lago Maggiore, Parte prima*. Società Geologica Italiana. Ed. Be-Ma.

Dal Piaz G.V., Del Moro A., Martin S. & Venturelli G. (1988) - *Post-collisional magmatism in the Ortler-Cevedale massif (Northern Italy)*. Jb. Geol. B.-A., Wien, **131**, 533-551.

Dal Piaz G.V., Hunziker J.C. & Martinotti G. (1972) - *La Zona Sesia-Lanzo e l'evoluzione tettonico-metamorfica delle Alpi nordoccidentali interne*. Mem. Soc. Geol. It., **11**, 433-466.

Dal Piaz G.V., Hunziker J.C. & Martinotti G. (1973) - *Excursion to the Sesia Zone of the Schweiz. Mineralogische und Petrographische Gesellschaft from September 30th to October 3rd, 1973*. Schweiz. Mineral. Petrogr. Mitt., **53**, 477-490.

Dal Piaz G.V., Venturelli G. & Scolari A. (1979) - *Calc-alkaline to ultrapotassic postcollisional volcanic activity in the internal northwestern Alps*. Mem. Sci. Geol., **32**, 16.

Dal Piaz G.V. & Venturelli G. (1985) - *Brevi riflessioni sul magmatismo post-ofiolitico nel quadro dell'evoluzione spazio-temporale delle Alpi*. Mem. Soc. Geol. It., **26**, 5-19.

Elliott T. (2003) - *Tracers of the slab*. In: Eiler J. (Eds.), *Inside the subduction factory*. Geoph. Monog. Series, **138**, 23-45.

Elliott T., Plank T., Zindler A., White W. & Bourdon B. (1997) - *Element transport from slab to volcanic front at the Mariana arc*. J. Geophy. Res.-Solid, **102**, 14991-15019.

Faccenna C., Funiciello F., Giardini D. & Lucente P. (2001) - *Episodic back-arc extension during restricted mantle convection in the Central Mediterranean*. Earth Planet. Sc. Lett., **187**, 105-116.

Ferrando S., Frezzotti M.L., Petrelli M. & Compagnoni R. (2009) - *Metasomatism of continental crust during subduction: the UHP whiteschists from the Southern Dora-Maira Massif (Italian Western Alps*. J. Metam. Geol., 27, 739-756.

Foley S.F. (1992) - *Vein-plus-wall-rock melting mechanisms in the lithosphere and the origin of potassic alkaline magmas*. Lithos, **28**, 435-453.

Foley S.F. Venturelli G., Green D.H. & Toscani L. (1987) - *The ultrapotassic rocks: characteristics, classification and constraints for petrogenetic models*. Earth-Sci. Rev., **24**, 81-134.

Fraser K.J., Hawkesworth C.J., Erlank A.J., Mitchell R.H. & Scott-Smith B.H. (1985) - *Sr, Nd and Pb isotope and minor element geochemistry of lamproites and kimberlites*. Earth Planet. Sc. Lett., **76**, 57-70.

Freymuth H., Elliott T., van Soest M. & Skora S. (2016) - *Tracing subducted black shales in the Lesser Antilles arc using molybdenum isotope ratios*. Geology, **44**(12), 987-990.

Freymuth H., Vils F., Willbold M., Taylor R.N. & Elliott T. (2015) - *Molybdenum mobility and isotopic fractionation during subduction at the Mariana arc*. Earth Planet. Sc. Lett., **432**, 176-186.

Gale A., Dalton C.A., Langmuir C.H., Yongjun S. & Schilling J.-G. (2013) - *The mean composition of oceanic ridge basalts*. Geochem. Geophy. Geosy., **14**(**3**).

Gebauer D., Schertl H.P., Brix M. & Schreyer W. (1997) - *35 Ma old ultrahigh-pressure metamorphism and evidence for very rapid exhumation in the Dora Maira Massif, Western Alps*. Lithos, **41**, 5-24.

Gao Y., Hou Z., Kamber B.S., Wei R., Meng X. & Zhao R. (2007) - *Lamproitic rocks from a continental collision zone: evidence for recycling of subducted Tethyan oceanic sediments in the mantle beneath Southern Tibet*. J. Petrol. **48**, 729-752.

Hein J.R., Koschinsky A. & Halliday A.N. (2003) - *Global occurrence of tellurium-rich ferromanganese crust and model for the enrichment of tellurium*. Geochim. Cosmochim. Ac., **67**, 1117-1127.

Kendall B., Dahl T.W. & Anbar A.D. (2017) - *The stable isotope geochemistry of molybdenum*. Rev. Mineral. Geochem., **82**(1), 683-732.

König S., Willie M., Voegelin A. & Schoenberg R. (2016) - *Molybdenum isotope systematics in subduction zones*. Earth Planet. Sc. Lett., **447**, 95-102.

Krmíček L., Romer R.L., Ulrych J., Glodny J. & Prelević, D. (2016) - *Petrogenesis of orogenic lamproites of the Bohemian Massif: Sr-Nd-Pb-Li isotope constraints for Variscan enrichment of ultra-depleted mantle domains*. Gondwana Res., **35**, 198-216.

Li Y., & Audétat A. (2012) - *Partitioning of V, Mn, Co, Ni, Cu, Zn, As, Mo, Ag, Sn, Sb, W, Au, Pb, and Bi between sulfide phases and hydrous basanite melt at upper mantle conditions*. Earth Planet. Sc. Lett., **355**, 327-340.

Lepore G.O., Bindi L., Pedrazzi G., Conticelli S. & Bonazzi P. (2017) - *Structural and chemical variations in phlogopite from lamproitic rocks of the Central Mediterranean Region*. Lithos, **286-287**, 191-205.

Mattei M., Petrocelli V., Lacava D. & Schiattarella M. (2004) - *Geodynamic implications of Pleistocene ultra-rapid verticalaxis rotations in the Southern Apennine (Italy)*. Geology, **32**, 789-792.

McLennan S.M. (2001) - *Relationships between the trace element composition of sedimentary rocks and upper continental crust*. Geochem. Geophy. Geosy., **2**, 1525-2027.

McManus J., Berelson W.M., Severmann S., Poulson R.L., Hammond D.E., Klinkhammer G.P. & Holm C. (2006) - *Molybdenum and uranium geochemistry in continental margin sediments: Paleoproxy potential.* Geochim. Cosmochim. Ac., **70**, 4643-4662.

Mirnejad H., & Bell K. (2006) - *Origin and source evolution of the Leucite Hills lamproites: evidence from Sr-Nd-Pb-O isotopic compositions*. J. Petrol., **47**(12), 2463-2489.

Mitchell R.H. & Bergman S.C. (1991) - *Potassic rocks and the lamproite clan*. In: *Petrology of Lamproites*. Springer, Boston, 9-38.

Montoya-Pino C., Weyer S., Anbar A.D., Pross J., Oschmann W., van de Schootbrugge B. & Arz H.W. (2010) - *Global enhancement of ocean anoxia during Oceanic Anoxic Event 2: A quantitative approach using U isotopes*. Geology, **38**, 315-318.

Murphy D.T., Collerson K.D. & Kamber B.S. (2002) - *Lamproites from Gaussberg, Antarctica: possible transition zone melts of Archaean subducted sediments*. J. Petrol., **43**, 981-1001.

Nelson D.R., McCulloch M.T. & Sun S.-S. (1986) - *The origins of ultrapotassic rocks as inferred from Sr, Nd and Pb isotopes.* Geochim. Cosmochim. Ac., **50**, 231-245.

Newsom H., White W., Jochum K. & Hofmann A. (1986) - *Siderophile and chalcophile element abundances in oceanic basalts, Pb iso-tope evolution and growth of the Earth's core.* Earth Planet. Sc. Lett., **80**, 299-313.

Noordmann J., Weyer S., Montoya-Pino C., Dellwig O., Neubert N., Eckert S., Paetzel M. & Böttcher M.E. (2015) - *Uranium and molybdenum isotope systematics in modern euxinic basins: Case studies from the central Baltic Sea and the Kyllaren fjord (Norway)*. Chem. Geol., **396**, 182-195.

Owen J.P. (2008) - *Geochemistry of lamprophyres from the Western Alps, Italy: implications for the origin of an enriched isotopic component in the Italian mantle*. Contrib. Mineral. Petr., **155**, 341-362.

Peccerillo A. & Frezzotti M.L. (2015) - Magmatism, mantle evolution and geodynamics at the converging plate margins of Italy. J. Geol. Soc., **172**, 407-427.

Peccerillo A. & Martinotti G. (2006) - *The Western Mediterranean lamproitic magmatism: origin and geodynamic significance*. Terra Nova, **18**, 109-117.

Peccerillo A. & Taylor S.R. (1976) - *Geochemistry of Eocene calc-alkaline volcanic rocks from the Kastamonu area, northern Turkey*. Contrib. Mineral. Petrol., **58**, 63-81.

Peccerillo A., Poli G. & Serri G. (1988) - *Petrogenesis of orenditic and kamafugitic rocks from Central Italy.* Can. Mineral., **26**, 45-65.

Plank T. (2005) - *Constraints from thorium/lanthanum on sediment recycling at subduction zones and the evolution of the continents*. J. Petrol., **46**, 921-944.

Prelević D., Foley S.F., Cvetković V. & Romer R.L. (2004) - *Origin of minette by mixing of lamproite and dacite magmas in Veliki Majdan, Serbia*. J. Petrol., **45**(4), 759-792.

Prelević D., Foley S.F., Romer R.L., Cvetković V. & Downes H. (2005) - *Tertiary ultrapotassic volcanism in Serbia: constraints on petrogenesis and mantle source characteristics.* J. Petrol., **46**, 1443-1487.

Prelević D., Foley S.F., Romer R.L. & Conticelli S. (2008) - *Mediterranean Tertiary lamproites derived from multiple source components in postcollisional geodynamics.* Geochim. Cosmochim. Ac., **72**, 2125-2156.

Prelević D., Stracke A., Foley S.F., Romer R. & Conticelli S. (2010) - *Hf isotope compositions of Mediterranean lamproites: mixing of melts from asthenosphere and crustally contaminated mantle lithosphere.* Lithos, **119**, 297-312.

Richards J.P. (2015) - *Tectonic, magmatic, and metallogenic evolution of the Tethyan orogen: from subduction to collision*. Ore Geol. Rev., **70**, 323-345.

Romaniello S.J., Herrmann A.D. & Anbar A.D. (2013) - *Uranium concentrations and U-238/U-235 isotope ratios in modern carbonates from the Bahamas: Assessing a novel paleoredox proxy*. Chem. Geol., **362**, 305-316.

Siebert C., Nägler T.F., von Blanckenburg F. & Kramers J.D. (2003) - *Molybdenum isotope records as a potential new proxy for paleoceanography*. Earth Planet. Sc. Lett., **211**, 159-171.

Skora S., Freymuth H., Blundy J., Elliott T. & Guillong M. (2017) - *An experimental study of the behaviour of cerium/molybdenum ratios during subduction: implications for tracing the slab component in the Lesser Antilles and Mariana Arc*. Geochim. Cosmochim. Ac., **212**, 133-155.

Soder C., Altherr R. & Romer R.L. (2016) - *Mantle metasomatism at the edge of a retreating subduction zone: Late Neogene lamprophyres form the Island of Kos, Greece.* J. Petrol., **57**, 1705-1728.

Stirling C.H., Andersen M.B., Potter E.K. & Halliday A.N. (2007) - *Low-temperature isotopic fractionation of uranium.* Earth Planet. Sc. Lett., **264**, 208-225.

Sun S.S. & McDonough W.S. (1989) - *Chemical and isotopic systematics of oceanic basalts: implications for mantle composition and processes*. Geol. Soc. Spec. Publ., **42**, 313-345.

Taylor S.R. & McLennan S.M. (1985) - *The continental crust: its composition and evolution: an examination of the geochemical record preserved in sedimentary rocks*. Oxford, Blackwell Scientific.

Tissot F.L. & Dauphas N. (2015) - *Uranium isotopic compositions of the crust and ocean: Age corrections, U budget and global extent of modern anoxia.* Geochim. Cosmochim. Ac., **167**, 113-143.

Tommasini S., Avanzinelli R. & Conticelli S. (2011) - *The Thorium/Lanthanum conundrum of the Tethyan realm lamproites: the role of recycled sediments and zoisite/lawsonite melting*. Earth Planet. Sc. Lett., **301**, 469-478.

Tribovillard N., Algeo T.J., Baudin F. & Riboulleau A. (2012) - *Analysis of marine environmental conditions based on molybdenum-uranium covariation - Application to Mesozoic paleoceanography*. Chem. Geol., **324-325**, 46-58.

Turner S.P., Platt J.P., George R.M.M., Kelley S.P., Pearson D.G. & Nowell G.M. (1999) - *Magmatism associated with orogenic collapse of the Betic-Alboran Domain, SE Spain.* J. Petrol., **40**(6), 1011-1036.

Venturelli G., Thorpe R.S., Dal Piaz G.V., Del Moro A. & Potts P.J. (1984) - *Petrogenesis of calc-alkaline, shoshonitic and associated ultrapotassic Oligocene volcanic rocks from Northwestern Alps, Italy*. Contrib. Mineral. Petrol., **86**, 209-220.

Von Blanckenburg F., Kagami H., Deutsch A., Oberli F., Meier M., Wiedenbeck M., Barth S. & Fischer, H. (1998) - *The origin of Alpine plutons along the Periadriatic Lineament*. Schweizerische Mineralogische und Petrographische Mitteilungen, **78**, 55-66.

Weyer S., Anbar A.D., Gerdes A., Gordon G.W., Algeo T.J. & Boyle E.A. (2008) - *Natural fractionation of $^{238}U/^{235}U$.* Geochim. Cosmochim. Ac., **72**, 345-359.

Willbold M. & Elliott T. (2017) - *Molybdenum isotope variations in magmatic rocks*. Chem. Geol., **449**, 253-268.

Willbold M., Hibbert K., Lai Y.J., Freymuth H., Hin R.C., Coath C., Vils F. & Elliott T. (2016) - *High-precision mass-dependent Molybdenum isotope variations in magmatic rocks determined by double-spike MC-ICP-MS*. Geost. Geoanal. Res., **40**, 389-403.

Manuscript received 18 December 2017; accepted 06 May 2018; published online 09 May 2018;
editorial responsibility and handling by A. Renzulli